COBEM 2023 27TH INTERNATIONAL CONGRESS OF MECHANICAL ENGINEERING

ABCM Brazilian Society of Mechanical Sciences and Engineering
27th ABCM International Congress of Mechanical Engineering
December 04-08, 2023, Florianópolis-SC, Brazil

COB-2023-1709
ASSESSMENT OF THE THERMO-HYDRAULIC PERFORMANCE OF FLOW IN CONCENTRIC ANNULAR ARRANGEMENT WITH THE INNER DIMPLED TUBE

Gustavo Lousado Silva
André Damiani Rocha
Laboratory of Simulation and Modeling on Energy Engineering, Federal University of ABC SP, Av. dos Estados, 5001, Santo André SP, Brazil
gustavo.lousado@aluno.ufabc.edu.br
a.damiani@ufabc.edu.br
William Monte Verde
Center for Energy and Petroleum Studies, University of Campinas, R. Cora Coralina, 350, Campinas SP, Brazil
wmv@unicamp.br

Abstract. *Flows of fluids in non-circular ducts like annular pipes are common in engineering equipment such as chemical mixing devices, turbomachinery, and drilling operations in the oil and gas industry. In thermal applications, such as solar heaters, heat exchangers, and electrical submersible pumps, the most widely used component in many heat transfer devices is an annuli tube, which transports the fluid to either gain or dissipate heat. Several options are available for enhancing heat transfer associated with internal flows and may be achieved by increasing the convection coefficient and/or introducing surface roughness to enhance turbulence. Previous investigations have shown that dimpled surfaces can improve heat transfer rate with relatively low-pressure loss compared to other heat transfer augmentation techniques. This paper presents a thermal-hydraulic flow assessment in a concentric annular arrangement with an inner dimpled tube through a computational fluid dynamics approach for a laminar flow regime. The numerical analysis has been carried out for axial Reynolds numbers less than 2000. Laminar flow numbers are chosen to emphasize applications where the working fluid is viscous. The effects of Reynolds and Prandtl numbers, dimple depth, radius, and pitch on thermal-hydraulic performance were computed. The ultimate aim of this study is to provide some guidelines for potential applications of enhanced heat transfer by dimples for viscous flows. Different temperature distribution patterns were found on the dimpled wall, and the performance is significantly affected by the pitch and the Prandtl number.*

Keywords: *Computational fluid dynamics (CFD), Heat transfer, Thermo-Hydraulic.*

1. INTRODUCTION

Energy consumption is increasing tremendously worldwide, which has economic and environmental consequences. It should be mentioned that a high amount of energy is consumed in the form of thermal energy in different sectors, including building energy systems, chemical vapor deposition facilities, electronic systems, solar energy systems, furnace engineering, etc. Efficient energy use has become very important to the world's sustainable development. There are several options for enhancing the efficiency of thermal systems (Webb et al., 2004). These options are classified into two groups, including active and passive techniques. The active technique is the one in which the energy is consumed to improve the efficiency of the thermal system, while the passive one does not consume any energy. Passive techniques are cost-effective and more trustworthy than active ones due to the absence of moving components. Some passive techniques used to improve the efficiency of thermal systems are flow disruption, secondary flows, surface roughness, re-entrant obstructions, channel curvature, and fluid additives. A brief literature review showed a large number of review papers about the applications of various passive techniques applied in different thermal energy systems. This shows the importance and privileged position of this topic for research communities. Passive heat transfer improvement methods are used to save energy and employ optimal energy resources. Usually, passive methods are associated with a flow resistance and pressure drop penalty. A proper technique of heat transfer improvement is needed to enhance the heat transfer considerably and reduce the pressure drop penalty as much as possible. Dimpled surfaces are recommended as a promising and popular passive heat transfer enhancement technique due to their low weight, small values of pressure drop penalty, simple fabrication, and small maintenance costs. Many experimental and numerical studies have been accomplished to investigate the potential of dimpled surface technology in various thermal energy systems.

Dimples are a particular form of surface roughness known formerly from golf ball aerodynamics (Ting, 2005). They are used on golf balls to decrease the flow resistance. Indeed, they produce a thin turbulent boundary layer of air, which adheres to the ball's wall. This leads to a smooth airflow on the ball's surface with low resistance. In thermal engineering

and energy systems, the dimpled surface technology is recognized as a promising passive technique because it can considerably augment the heat transfer rate with a low flow resistance penalty.

The local flow structures inside the dimples and mechanisms responsible for heat transfer improvement by dimples are shown in Figure 1. The flow can be separated, and recirculation flow can be formed in the upstream half of the dimples, where a very low heat transfer can occur. Moreover, the shear layer can be reattached from the back edge of the dimples, where a large amount of heat transfer can occur. The fluid experiences flow circulation in a wide area of the dimple. Upwash flow is generated after the incoming advection-mixed-impingement. After that, this upwash flow and the approaching impinging flow can mix and form a mixed flow, passing the next dimple.

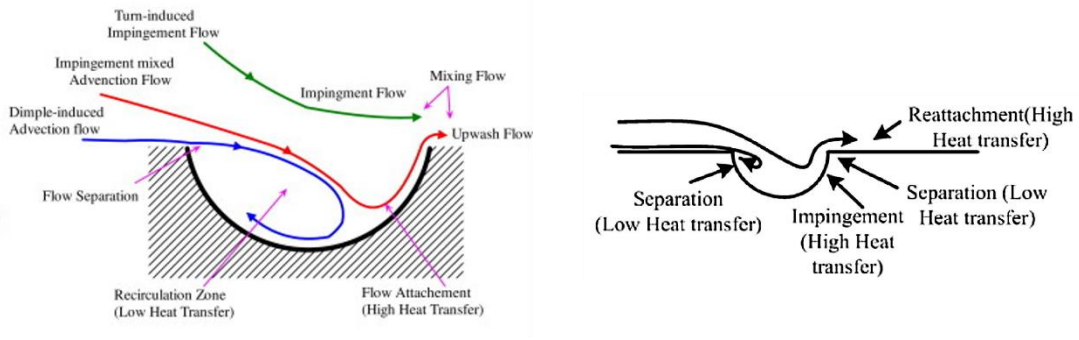

(a) (b)

Figure 1. Heat transfer improvement by dimples: (a) conceptual plot (Xie and Sundén, 2010) and (b) mechanisms responsible for heat transfer (Luo et al., 2017).

As shown in Figure 1, large velocity vectors are generated around the dimple's downstream region; a high heat transfer rate can occur in this region. It should be mentioned that the local heat transfer at the downstream regions of the dimples can be enhanced due to the actions of the upright flow shedding from the dimples, consisting of a big upwash area with layers of fluid exiting from the core area of each dimple, and also vortex pairs are shed from the dimple diagonals (Ligrani et al., 2001). These are the main factors responsible for dimple's convective heat transfer improvement. Accordingly, the main factors are flow reattachment, flow impingement, and upwash flow at the downstream region of the dimples. Moreover, the heat transfer rate at the upstream region of the dimples is low due to the separation and recirculation of flow in this region.

2. LITERATURE REVIEW

There are some studies about the influences of the geometry and arrangements of dimples on flow structures and heat transfer in dimples. Although there are many results for external turbulent flows (flow over dimpled surfaces), this work focuses on internal laminar flows. The studies on different geometries and arrangements of dimples for the internal flows through channels or ducts with dimpled surfaces are presented in this section.

In an experimental study, Morcos (1988) investigated the efficiency of a shell-and-dimpled tube heat exchanger in the recovery of the lost heat and observed that for counter-flow, a dimpled heat exchanger gives 80% and 35% higher heat transfer coefficient and effectiveness, respectively, than a smooth one. However, for the parallel flow, a dimpled heat exchanger provides 55% and 25% higher heat transfer coefficient and effectiveness than a smooth one. Khalatov et al. (2004) studied the water flow over spherical and cylindrical dimples for the Reynolds (based on dimple diameter) number lower than 25,000 in the laminar and turbulent regimes in rectangular channels. Their results showed that for the Reynolds number lower than 10,000, there is no difference between the development of the in-dimple separation zone of cylindrical and spherical dimples. Generally, cylindrical dimples provide longer separation zones than spherical dimples at similar flow conditions. Borisov et al. (2004) investigated the heat transfer and pressure drop of airflow through rectangular channels in both the laminar and turbulent ($770 < Re < 26{,}500$). They used two kinds of heat transfer enhancement methods, including dimple concavities and combining dimples on one side with concentrically arranged toroidal banks protruding into the duct on the other side. They concluded that the heat transfer improvement factor in the duct with one dimpled side and another banked side at 73% is reaching 4.3 compared to the improvement of 3.7 for a high-density (67%) double-sided dimpled passage. The corresponding friction factor for the investigated dimple-bank configuration reaches 27 compared to 2.3 for the dimpled duct.

Wei et al. (2007) simulated the airflow and heat transfer through a microchannel with one dimpled surface. They concluded that the dimples could improve the heat transfer for laminar flows in the microchannels. They observed that the maximum heat transfer improvement could occur around the downstream edge of the dimple. The pressure drop of the laminar flow in the dimpled microchannel is either equivalent to or less than the pressure drop produced in a smooth microchannel. Elyyan and Tafti (2009) used some new split dimples as the surface roughness on an interrupted plate fin.

The split dimples continuously perturb the boundary layer formed on the fin surface and generate energetic shear layers, which provide an extra mechanism for heat transfer enhancement achieved by dimples. The sizes of these recirculating flows are smaller for laminar flow at a Reynolds number of 240. These recirculating flows disrupt the thermal boundary layer formed on the fin surface and improve the turbulence intensities in the flow field and heat transfer from the fin.

Lan et al. (2012) studied the influences of leading edge boundary layer thickness on the dimple flow structure in a microchannel under laminar water flow conditions (100 < Re < 900). They observed that the active vortices are formed further downstream by increasing the ratio of leading-edge boundary layer thickness to dimple depth. Isaev et al. (2015) increased the heat transfer in a narrow channel under laminar-turbulent water flow conditions (100 < Re < 20,000) with one-row oval dimples. They considered stepwise and zigzag arrangements of the dimples. They found that the best case is a zigzag relief with shifted dimples that provides heat transfer intensification of 90% and 25% increment in the hydraulic loss compared to the plane-parallel channel. Liu and Sakr (2013) performed a literature review on the passive heat transfer improvement techniques in pipe heat exchangers. They concluded that the twisted tape inserts act better in a laminar regime than in a turbulent one. However, the other passive methods, including ribs, conical nozzle, conical ring, etc., are generally better in turbulent flow than the laminar one. Liang et al. (2017) investigated the thermal-hydraulic performance of ellipsoidal dimpled tubes. It was observed that the dimple arrangement significantly affected the heat transfer rate. For Re < 104, the ellipsoidal dimples with a major axis aligned to the flow direction (i.e., ellipsoidal 0°) resulted in the highest heat transfer rate.

The literature review shows that most of the studies carried out to date are related to rectangular canals. In circular section tubes, the studies are concentrated on shell and tube or coaxial heat exchangers for turbulent flow. The researchers used fluids with a low Prandtl number (Pr ~ 1). In high-viscosity fluids (Pr >> 1), such as hydrocarbon fluids, the thermo-hydraulic performance has not yet been investigated in depth. Examples of operation with high-viscosity fluids include heavy oil fields and liquid-liquid mixtures forming when water is present. One of the essential aspects of heavy oils is that their viscosity directly impacts the reservoir's recovery, productivity, separation process, and transportation methods.

The main objective of the present study is to provide a numerical prediction on flow characteristics and heat transfer performances for an annular tube with a dimpled inner heated wall, using spherical dimples in a staggered configuration, at Reynolds number ranging from 500 to 2000 and Prandtl number ranging from 80 to 1500. The thermal-hydraulic performance is investigated based on CFD simulations. The effects of dimple depth and dimple radius on thermal-hydraulic performance are investigated. The aim of this study is to provide some guidelines for potential applications of dimpled walls in viscous flows.

3. PHYSICAL MODEL AND NUMERICAL METHOD

The three-dimensional model of a quarter computational annular tube is shown in Figure 2. The computational domains consist of a tube of hydraulic diameter d_h with radius aspect ratio of 0.5. The spherical dimples with radius R, depth D, longitudinal pitch P_z and circumferential pitch P_θ are equidistantly mounted of the smooth inner wall in staggered configuration, as shown in Figure 3. The size of spherical dimple for different simulation cases are present in Table 1.

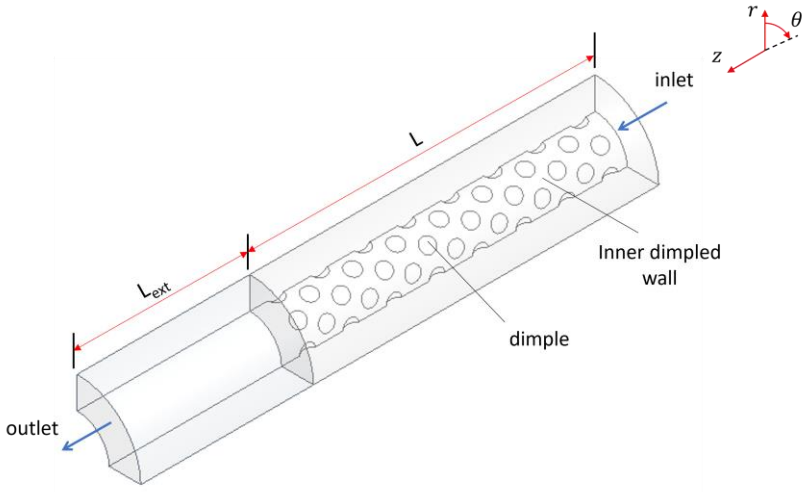

Figure 2. Three-dimensional domain.

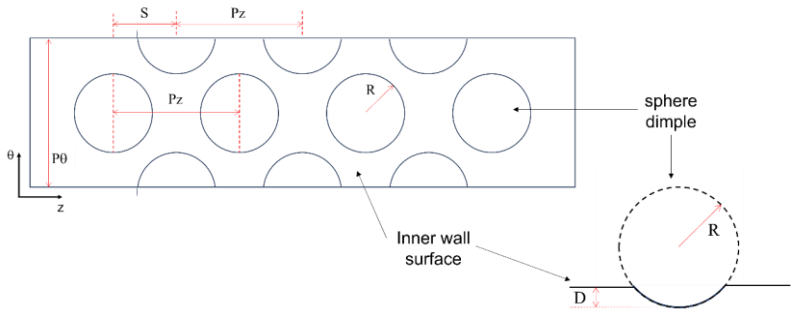

Figure 3. Details of the inner dimpled wall.

Table 1. Geometric parameters for spherical dimples.

Case	R (mm)	D (mm)	P_z (mm)	P_θ (°)
Case A	30	1, 3, 5	125	30
Case B	10, 20, 30	3	125	30
Case C	30	3	50	30

The flow is assumed to be a steady-state, incompressible, and laminar, with constant fluid properties and negligible viscous dissipation. With these simplifications, continuity, momentum, and energy equations are written in vector form as,

$$\nabla \cdot \vec{u} = 0 \tag{1}$$

$$\vec{u} \cdot \nabla \vec{u} = -\frac{1}{\rho}\nabla p + \nu \nabla^2 \vec{u} \tag{2}$$

$$\vec{u} \cdot \nabla T = \alpha \nabla^2 T \tag{3}$$

where $\vec{u}$ is the velocity vector, T is temperature, ρ, ν, α are density, kinematic viscosity, and thermal diffusivity, respectively.

The annular test section length of the main domain is L. An additional outlet extent length of L_{ext} size is used to ensure the outlet does not influence the main domain. Velocity distribution at the inlet was assumed to be uniform. At the outlet, pressure outlet boundary condition was used. At the walls, no-slip conditions were specified. The uniform heat flux of $10^3\, W/m^2$ was specified at the inner dimpled wall, while the other walls are set with adiabatic. On the sides, the symmetry condition was specified.

4. PARAMETERS DEFINITIONS

Reynolds number (Re) is a dimensionless number, defined as the ratio of inertial to viscous forces,

$$Re = \frac{\rho V_b\, d_h}{\mu} \tag{4}$$

where V_b is the bulk velocity and d_h is the hydraulic diameter. The convective heat transfer coefficient (h) is a ratio of heat flux to logarithmic mean temperature difference,

$$h = \frac{q}{\Delta T} \tag{5}$$

where q is the wall heat flux, ΔT is the log mean temperature difference between the heating wall and cooling flow. In this equation, the ΔT is defined as,

$$\Delta T = \frac{(T_w - T_{in}) - (T_w - T_{out})}{\ln\left[\frac{(T_w - T_{in})}{(T_w - T_{out})}\right]} \tag{6}$$

where T_w is the temperature of the wall, T_{in} is the inlet fluid temperature and T_{out} is the out fluid temperature. The ratio of convective heat transfer to the conductive heat transfer of a fluid is represented by a non-dimensional average Nusselt number ($\overline{Nu}$), which was average determined as,

$$\overline{Nu} = \frac{hd_h}{k} \tag{7}$$

where k is the thermal conductivity of the fluid. The Darcy friction factor (f) was used to determine the hydraulic loss of the tube flow,

$$f = \frac{2\Delta p d_h}{\rho V_b^2 L} \tag{8}$$

where Δp is the pressure drop for the test section, and L is the length of the test section.

Performance Evaluation Criteria (PEC) is the ratio of heat transfer enhancement to hydraulic losses and is commonly defined as Eq. (9). The heat transfer enhancement is associated with the ratio of Nusselt number of enhanced tube and smooth tube, while the hydraulic losses are associated with the ratio of friction factor of enhanced tube and smooth tube. When PEC > 1, the comprehensive heat transfer performance of the dimple tube is higher than that of the smooth tube, therefore, this criterion embeds both traditional indicators for the heat transfer assessment hydraulic performance estimators.

$$PEC = \frac{\overline{Nu}/\overline{Nu_0}}{(f/f_0)^{1/3}} \tag{9}$$

5. NUMERICAL METHOD AND GRID INDEPENDENCE STUDY

The governing equations were discretized and solved by using the cell-centered finite volume method. The diffusion term was approximated using the second-order central difference, while the second-order upwind scheme was adopted to approximate convection terms. The coupled algorithm was adopted for solving pressure-velocity coupling equations, and commercial CFD software Ansys Fluent® was used for the numerical calculations. The polyhedral mesh was adopted for the computational domain. The mesh is refined in the wall and entrance regions, using a low growth rate. The iterations were continued until the residuals of continuity and momentum equations were reduced below $10^{-6,}$ and the energy equation was reduced below 10^{-9}. The numerical convergence was monitored by calculating the bulk temperature in three axial locations and through the maximum temperature of the dimpled wall. The mesh independence study was conducted for Re = 2000, Pr = 1500, r* = 0.5, R = 10 mm, D = 3 mm, P_θ = 30° and Pz = 125 mm. The results for average Nusselt number and the Darcy friction factor are presented in Table 2. The number of cells for different mesh sizes varied from 0.15 million (coarse mesh) to 8.21 million (fine mesh). The relative difference between Grid 5 and Grid 6 was 2.4% and 0.02% for the Nusselt number and friction factor, respectively. Therefore, Grid 6 was chosen for simulations in this work.

Table 2. Grid independence study

Grids	Cells (Million)	$\overline{Nu}$	f
1	0.15	154.9856	0.16116
2	0.33	212.8263	0.15437
3	0.72	264.1594	0.15040
4	1.63	302.8190	0.14821
5	3.67	319.1655	0.14748
6	8.21	311.6094	0.14751

6. RESULTS AND DISCUSSION

6.1. Validation

To ensure the accuracy of present numerical results, the numerical model employed in the simulation should be validated first. Accordingly, the numerical results of smooth annuli pipe are compared with fRe data reported by Shah and Farnia (1974), tabulated by Liu (1974), in Figure 4a, and local Nusselt number data reported by Heaton et al. (1964) in Figure 4b. The maximum difference between the numerical results and literature data for friction factor and local

Nusselt number was found to be less than 7% and 2.5%, respectively. Due to the structure of the enhanced annuli tube with dimples being more complex than the smooth annuli tube, the numerical and experimental results should be compared. However, this validation has not been carried out to date. However, the agreement between the numerical results and literature indicates the reliability of the computational model, and it confirmed the simulation methods adopted are correct in this study.

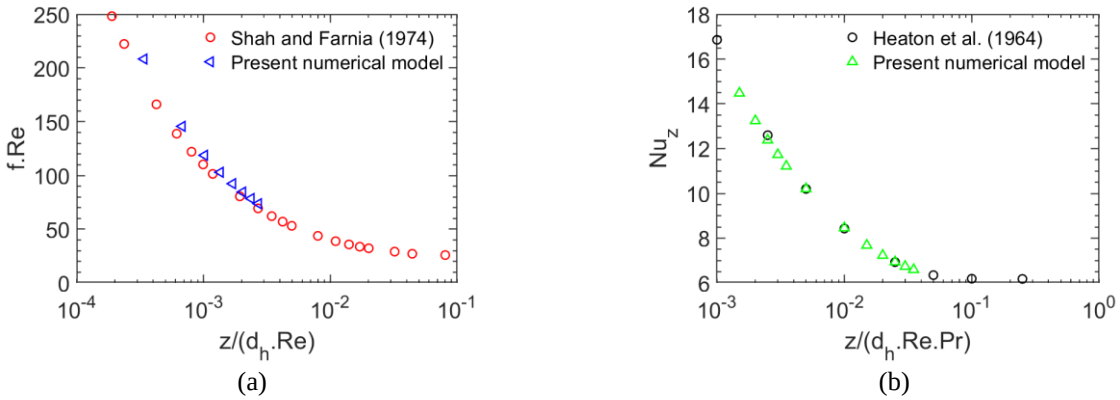

Figure 4. Validation for friction factor and local Nusselt number for smooth annuli tube.

6.2. Flow Field

The following results are presented using the row and column definitions, as shown in Figure 5. Due to the staggered configuration, the odd lines have four dimples, and the even lines have three. The local structure of the flow field is shown in Figure 6 at a different axial distance (different rows) of the dimpled wall. The local structure of the flow field changes in the axial direction, and one can observe vortex pairs formed on the sides (based on the flow direction) of each dimple, with slight asymmetry. Although the dimple is symmetrical, non-symmetrical flow patterns are evident within the dimple (highlighted on the right).

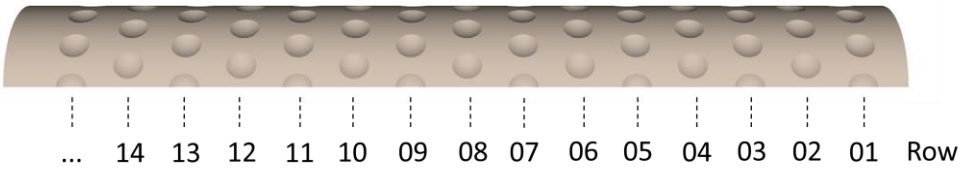

Figure 5. Definition of rows of dimples.

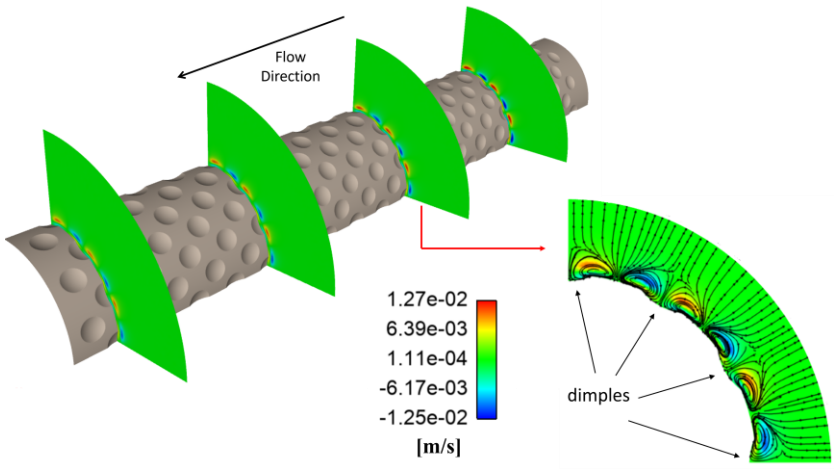

Figure 6. Contour of tangential velocity for different rows and streamlines, at z = 0.5 m, for Case C.

The pairs of vortices formed on the sides, highlighted in Figure 6, lead to a negative radial velocity in the center of the dimple region, which means it is a jet impingement flow, as shown in Figure 7. The tangential and radial components of velocities decrease in magnitude as z increases, and the flow becomes approximately purely axial.

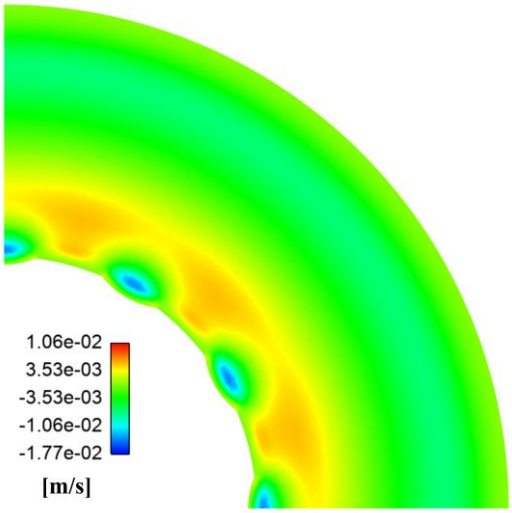

Figure 7. Contours of radial and tangential velocity, at z = 0.5 m, for Case C.

The flow structure close to the dimpled wall will dictate the disturbance of the boundary layer and, consequently, the heat transfer. The temperature increases with increasing axial distance z for the smooth, heated wall, as shown in Figure Xa. Figure 9 compares the temperature on the heated dimpled wall of Case A with D = 5 mm and C with smooth wall. Under the condition of constant wall heat flux, it is expected, for the smooth wall, that the wall temperature is higher at the end of the tube when z → L. The maximum temperature in the smooth wall is approximately 98°C (Figure 8a). The dimpled wall's boundary layer is disturbed by dimples, impacting heat transfer and temperature distribution. Figure 8b shows a different temperature distribution pattern than the smooth wall, containing hot spots, because this configuration (Case A) has greater depth dimples. The maximum temperature for this configuration is 141°C. When the dimple depth and spacing are smaller (Case C), the maximum temperature obtained is 124°C, as shown in Figure 8c.

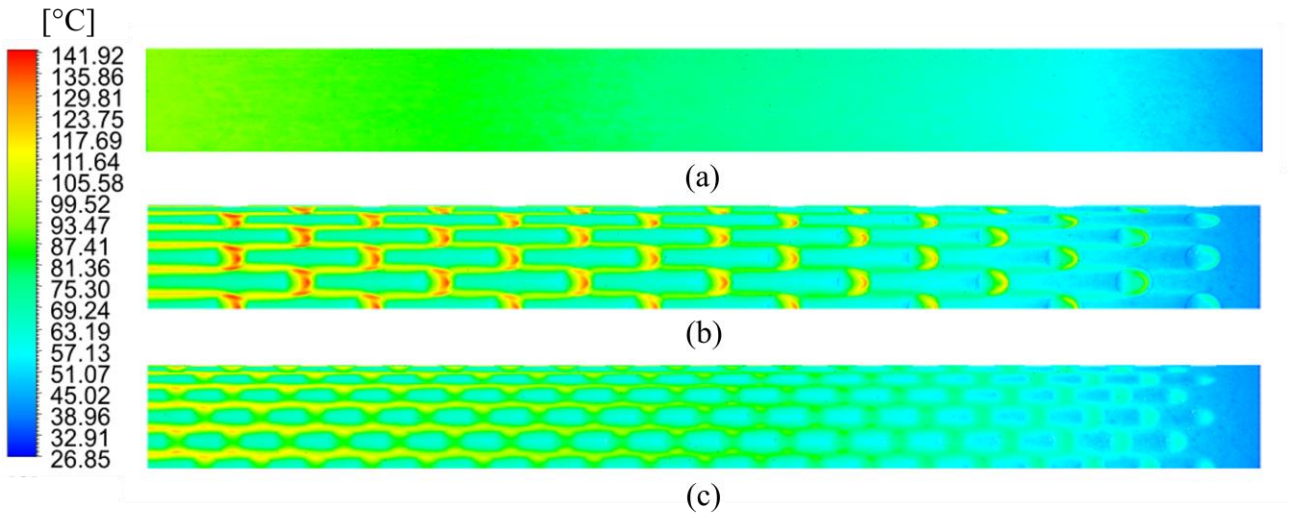

Figure 8. Contours of temperature: (a) smooth wall, (b) Case A with D = 5 mm, and (c) Case C.

6.3. Thermo-hidraulic performance

The effect of dimple depth on thermal-hydraulic performance is present in Figure 9 for Pr = 1500. Figure 9a presents friction factor increment with Re, as a function of depth (D), for R = 30 mm, θ = 30° and Pz = 125 mm. The friction factor decreases with increasing Reynolds number, as expected. No significant variation of friction factor was found for the

investigated depths. The variations of the heat transfer enhancement factor with Re for different D are shown in Figure 9b. The average Nusselt number increases with increasing Reynolds number, and the average Nusselt number for D = 1mm is slightly larger than D = 3 mm and D = 5 mm. For D = 1 mm, the mean Nusselt number was approximately 314.86. Figure 10c shows the thermal performance with Re for different D. The PEC increases with an increase of Re and a decrease of D. The highest PEC is associated with the smallest depths (D = 1 mm and D = 3 mm). The maximum PEC is 1, obtained by D = 1 mm when Re = 2000. For all ranges of Reynolds number, the PEC is smaller than unity for D = 5 mm.

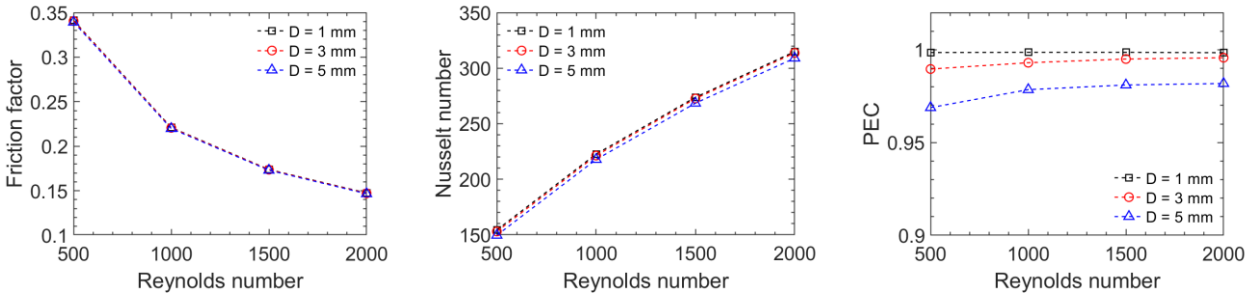

Figure 9. Effect of dimple depths on thermal-hydraulic performance for Case A.

The effect of dimple radius on thermal-hydraulic performance is present in Figure 10, for D = 3 mm, θ = 30°, Pz = 125 mm, and Pr = 1500. No significant variation for friction factor and Nusselt number was found for the investigated radius (Figures 10a and 10b). The PEC is about 1, obtained by R = 30 mm when Re = 2000, as shown in Figure 10c. For Reynolds number equal to 500, the PEC is smaller than unity for all configurations of Case B. Figures 9 and 10 show that performance is moderately dependent on depth and weakly dependent on dimple radius.

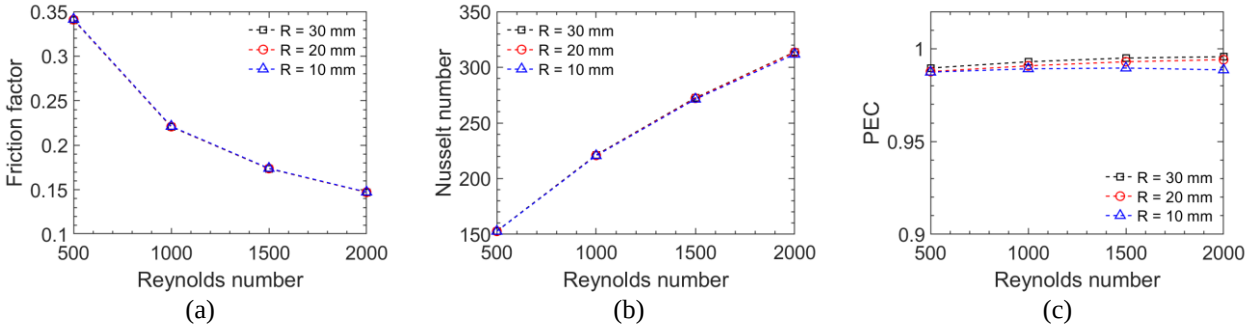

Figure 10. Effect of radius on thermal-hydraulic performance for Case B

Figure 11 shows the influence of axial pitch on thermal-hydraulic performance for D = 3 mm and θ = 30°. There is no significant variation for friction factor (Figure 11a), but the Nusselt number is higher for the smallest pitch (Figure 11b). This behavior leads to an increase in PEC, as shown in Figure 11c, greater than 1.

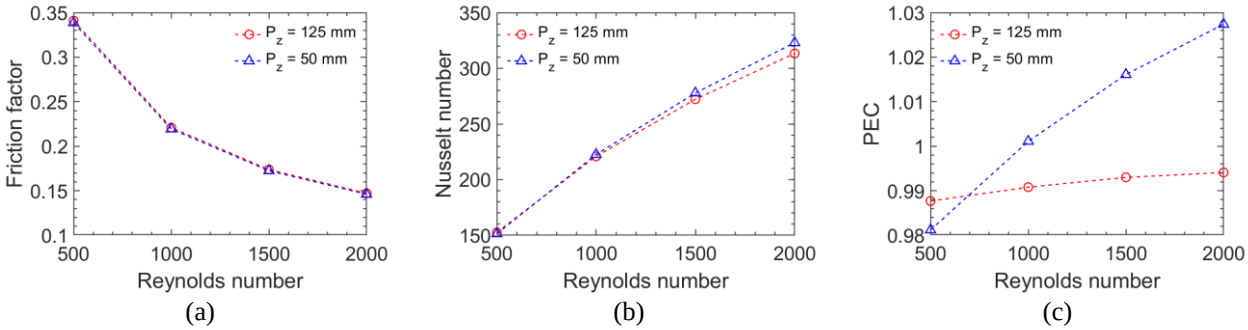

Figure 11. Effect of axial pitch on thermal-hydraulic performance (D = 3 mm, θ = 30° – Cases B and C).

Figure 12 summarizes the PEC for all cases defined in Table 1. The lowest PEC value found was 0.97 for Case A with D = 5 mm, for Re = 500. The maximum PEC value was 1.027 for Case C with Pz = 50 mm, for Re = 2000. Case C presents a PEC > 1 from Re = 1000. From this result, it is possible to conclude that the PEC is sensitive to axial pitch and increases with decreasing of the pitch. On the other hand, the result also shows that the PEC decreases with increasing dimple depth.

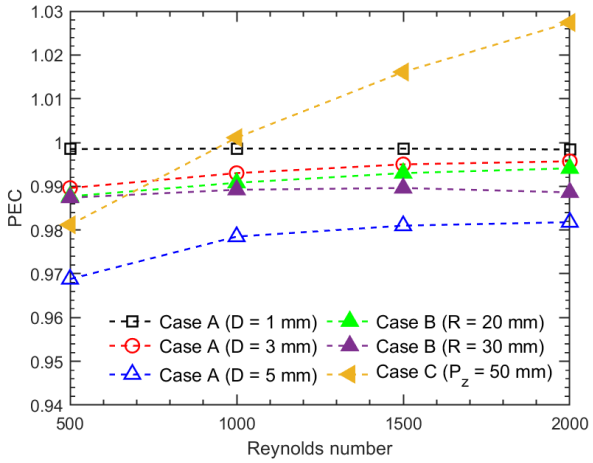

Figure 12. The Performance Evaluation Criteria (PEC) for all cases.

Figure 13 presents the effect of the Prandtl number on PEC for Case A (Re = 2000, R = 30 mm, D = 3mm, θ = 30°, Pz = 125 mm). The PEC decreases smoothly with the decrease of the Prandtl number. This result only indicates a trend of this effect. This result suggests that thermo-hydraulic performance should improve with increasing Prandtl number. Unlike the literature, this result shows the potential applications of the dimpled annuli tube in the laminar tube flow regime for viscous fluids. As the thermal entry region is larger when the Prandtl number is higher, this result is particularly important for long tubes.

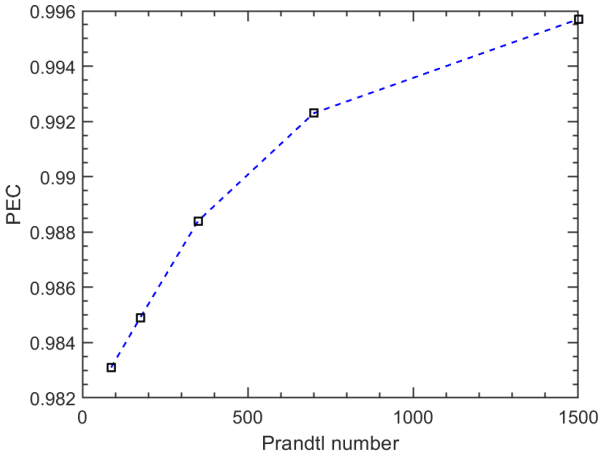

Figure 13. PEC *versus* Pr.

7. CONCLUSIONS

Laminar forced convection heat transfer was investigated numerically to obtain the thermal-hydraulic flow assessment in a dimpled inner wall of an annular tube for different Reynolds numbers, Prandtl numbers, dimple's depth, radius, and pitch. Despite the geometric symmetry of the cavity, the flow over it is slightly asymmetrical, and pairs of vortices are formed on the sides of the dimple, disturbing the boundary layer. Different temperature distribution patterns were identified. Case C presented the lowest temperature and the highest PEC values among the cases with dimpled walls. The performance of shallow dimples is greater than that of deep dimples, and the influence of radius on performance is very small. The parameter with the greatest influence on the PEC was the pitch, as shown in Figure 11c. In this case, the PEC was found to be greater than unity from Re = 1000. This paper's significant contribution was that the performance is

higher for viscous fluid under a laminar flow regime. The Prandtl number affects the performance, indicating its potential application in systems operating with viscous fluids.

8. REFERENCES

Barrios, L., Rojas, M., Monteiro, G., Sleight, N., 2017. Brazil field experience of ESP performance with viscous emulsions and high gas using multi-vane pump MVP and high power ESPs. In: Society of Petroleum Engineers - SPE Electric Submersible Pump Symposium, The Woodlands, Texas, USA.

Barrios, L., Scott, S., Rivera, R., Sheth, K., 2012. ESP technology maturation: Subsea boosting system with high GOR and viscous fluids. In: Proceedings - SPE Annual Technical Conference and Exhibition, San Antonio, Texas USA.

Borisov, I., Khalatov, A., Kobzar, S., Glezer, B., 2004. Comparison of thermo-hydraulic characteristics for two types of dimpled surfaces. Proceedings of the ASME Turbo Expo 2004, p. 1–10.

Correa, S., Iovane, M., Pinneri, S., 2021. Role of Electrical Submerged Pumps in Enabling Asphaltene-Stabilized Emulsions. Energy and Fuels, v. 30, n. 5, p. 3622- 3629.

Elyyan, M., Tafti, D., 2009. A novel split-dimple interrupted fin configuration for heat transfer augmentation. International Journal of Heat and Mass Transfer, v. 52, n. 5–6, p. 1561–1572.

Isaev, S. A., Leontiev, A. I., Kornev, N. V., Hasssel, E., Chudnovskii, Y. P., 2015. Heat transfer intensification for laminar and turbulent flows in a narrow channel with one-row oval dimples. High Temperature, v. 53, n. 3, p. 375–386.

Khalatov, A., Byerley, A., Ochoa, D., Min, S., 2004. Flow characteristics within and downstream of spherical and cylindrical dimple on a flat plate at low Reynolds numbers. Proceedings of the ASME Turbo Expo 2004, v. 3, p. 589–601.

Lan, J., Xie, Y. Zhang, D., 2012. Flow and heat transfer in microchannels with dimples and protrusions. Journal of Heat Transfer, v. 134, n. 2, p. 1–9.

Liang, Z., Xie, S., Zhang, L., Zhang, J., Wang, Y., Yin, Y., 2017. Influence of geometric parameters on the thermal hydraulic performance of an ellipsoidal protruded enhanced tube. Numerical Heat transfer, Part A, v. 72, n. 2, p. 153–170.

Ligrani, P. M., Harrison, J. L., Magmmod, G. I., Hill, M. L., 2001. Flow structure due to dimple depressions on a channel surface. Physics of Fluids, v. 13, n. 11, p. 3442–3451.

Liu, J., 1974. Flow of a Bingham fluid in the entrance region of an annular tube. Master of Thesis Dissertation, University of Wisconsin, Milwaukee.

Liu, S., Sakr, M., 2013. A comprehensive review on passive heat transfer enhancements in pipe exchangers. Renewable and Sustainable Energy Reviews, v. 19, p. 64–81.

Luo, L., Wen, F., Wang, L., Sundén, B., Wang, S., 2017. On the solar receiver thermal enhancement by using the dimple combined with delta winglet vortex generator. Applied Thermal Engineering, v. 111, p. 586–598.

Morcos, V. H., 1988. Performance of shell-and-dimpled-tube heat exchangers for waste heat recovery. Heat Recovery Systems and CHP, v. 8, n. 4, p. 299–308.

Patil, A., Morrison, G., 2019. Affinity law modified to predict the pump head performance for different viscosities using the Morrison number. Journal of Fluids Engineering, Transactions of the ASME, v. 141, n. 2.

Perissinotto, R. M., Monte Verde, W., Galassi, M., Gonçalves, G. F. N., Castro, M. S., Carneiro, J., Biazzussi, J. L., Bannwart, A. C., 2019. Experimental and numerical study of oil drop motion within an ESP impeller. Journal of Petroleum Science and Engineering, v. 175, p. 881- 895.

Shah, V. L., Farnia, K, 1974. Flow in the entrance of annular tubes. Computer and Fluids, v. 2, p. 285-294.

Ting, L. L., 2005. Some additional CFD flow field solutions showing the effect of teardrop shaped dimple design on the golf ball aerodynamic performance. Journal of Visualization, v. 8, n. 1, p. 4–4.

Trevisan, F. E., 2009. Modeling and Visualization of Air and Viscous Liquid in Electrical Submersible Pump. 2009. The University of Tulsa.

Trevisan, F., Prado, M., 2011. Experimental investigation of the viscous effect on two-phase-flow patterns and hydraulic performance of electrical submersible pumps. Journal of Canadian Petroleum Technology, v. 50, n. 4, p. 45- 52.

Webb, R. L., Sunden, B., Kim, N., 2007. Principles Enhanced Heat Transfer. Second Edition.

Wei, X. J., Joshi, Y. K., Ligrani, P. M., 2007. Numerical simulation of laminar flow and heat transfer inside a microchannel with one dimpled surface. Journal of Electronic Packaging, Transactions of the ASME, v. 129, n. 1, p. 63–70.

Xie, G., Sundén, B., 2010. Numerical predictions of augmented heat transfer of an internal blade tip-wall by hemispherical dimples. International Journal of Heat and Mass Transfer, v. 53, n. 25–26, p. 5639–5650.

RESPONSIBILITY NOTICE